# Simultaneous Missing Value Imputation and Structure Learning with Groups

**Pablo Morales-Alvarez**[*][†] University of Granada

**Wenbo Gong** Microsoft Research

**Angus Lamb**[†] G-Research

**Simon Woodhead** Eedi

**Simon Peyton Jones**[†] Epic Games

**Nick Pawlowski** Microsoft Research

**Miltiadis Allamanis**[†] Google

**Cheng Zhang** Microsoft Research

## Abstract

Learning structures between groups of variables from data with missing values is an important task in the real world, yet difficult to solve. One typical scenario is discovering the structure among topics in the education domain to identify learning pathways. Here, the observations are student performances for questions under each topic which contain missing values. However, most existing methods focus on learning structures between a few individual variables from the complete data. In this work, we propose VISL, a novel scalable structure learning approach that can simultaneously infer structures between groups of variables under missing data and perform missing value imputations with deep learning. Particularly, we propose a generative model with a structured latent space and a graph neural network-based architecture, scaling to a large number of variables. Empirically, we conduct extensive experiments on synthetic, semi-synthetic, and real-world education data sets. We show improved performances on both imputation and structure learning accuracy compared to popular and recent approaches.

## 1 Introduction

Understanding the structural relationships among different variables provides critical insights in many real-world applications, such as medicine, economics and education [42, 62]. Thus, learning graphs from observed data, known as structure learning, has recently made remarkable progress [10, 61, 63, 64].

For many applications, variables in the data can be gathered into semantically meaningful groups, where useful insights are at group level. For example, in finance, one may be interested in how a financial situation influences different industries (i.e. groups) instead of individual companies (i.e. variables). Similarly, in education, the data can contain student responses to thousands of individual questions (i.e. variables), where each question belongs to a broader topic (i.e. groups). Again, it is insightful to find relationships between topics instead of individual questions. Moreover, real-world data such as educational data is inherently sparse since it is not feasible to ask every question to every student; the dimensions of the data in terms of the number of variables and the number of observations are very high, posing a scalability challenge. Despite the progress in structure learning, no existing method can discover group-wise relationships given large-scale partially observed data.

In this work, we present VISL (missing value imputation with structural learning), a novel approach to simultaneously tackle group-wise structure learning and missing value imputations driven by the

[*] Department of Statistics and Operation Research, University of Granada, Spain

[†] Work done while internship in Microsoft Research Cambridge.

Correspondence to: Cheng Zhang <Cheng.Zhang@microsoft.com>

36th Conference on Neural Information Processing Systems (NeurIPS 2022).

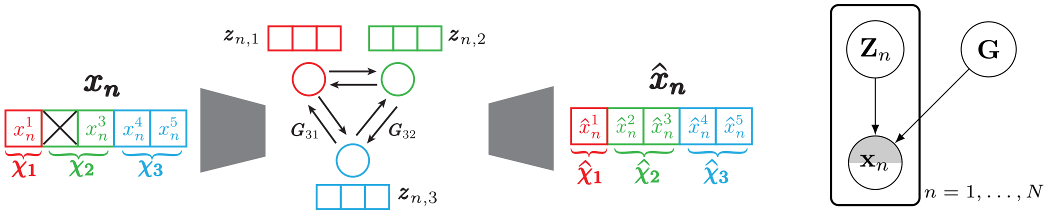

(a) (b)

Figure 1: (a) Graphic representation of VISL. VISL is a variational auto-encoder based framework. Observations from each group are encoded into low dimensional latent variables. The structure is treated as a global latent variable. A GNN based decoder is used to decode the latent variables to observations. (b) Probabilistic graphical model for VISL, where the partial observation $\mathbf{x}$ is generated from its local latent variable $\mathbf{z}$ and the global latent variable $\mathbf{G}$ which characterizes the structures.

real-world topic relationship discovery in an education setting. This is accomplished by combining variational inference with a generative model that leverages a structured latent space and a decoder based on message-passing Graph Neural Networks (GNN) [13]. Namely, the structured latent space endows each group of variables with its latent subspace, and the interactions between the subspaces are regulated by a GNN whose behavior depends on the inferred graph from variational inference, see Fig. 1(a). VISL satisfies all the desired properties: it leverages continuous optimization of the structure learning to achieve scalability [63, 64]; the VISL formulation naturally handles missing values, and it can discover relations at different levels of granularity with pre-defined groups. Empirically, we evaluate VISL on one synthetic and two real-world problems including the aforementioned education scenario. VISL shows improved performance in both missing data imputation and structure learning accuracy compared to popular and recent approaches for each task. We worked closely with an education domain expert to evaluate the learned topic relationships, and our model has provided insightful results as recognized by the domain experts.

## 2 Model Description

In the following, we present the formulation of VISL for scalable group-wise structure learning with partial observations using a novel deep generative model based framework.

### 2.1 Problem setting

Assume a training data set $\mathbf{X} = \{\mathbf{x}_n\}_{n=1}^{N}$ with $\mathbf{x}_n \in \mathbb{R}^D$. The observed and missing values are denoted as $\mathbf{X}_O$ and $\mathbf{X}_U$, respectively, where we assume the data are missing completely at random (MCAR) or missing at random (MAR). In Appx. A, we explain how to handle MAR. In particular, variables can be gathered into $M$ groups, where each can be denoted as $\boldsymbol{\chi}_{n,m} = [x_{n,i}]_{i \in \mathcal{I}_m}$. $\mathcal{I}_m$ containing the variable indices belonging to group $m$ (e.g., $\mathcal{I}_2 = [4, 5, 6]$ indicates group 2 includes the 4th, 5th and 6th variables). One should note that each $\mathcal{I}_m$ may have varying sizes for different $m$ (i.e. varying group sizes). Throughout the paper, we assume the group information is provided a priori. If this information is unavailable, casual representation learning can be leveraged to represent low-level signals into groups. The goal of VISL is to (i) perform missing value imputation for test samples and (ii) infer structures between groups of variables. We use the adjacency matrix $\mathbf{G} \in [0, 1]^{M \times M}$ to represent a graph, where $G_{ij} = 1$ or 0 indicates whether there is a directed edge from $i-$th to $j-$th group or not. In the context of the education domain, the above formulation can be rephrased as follows: variable $\mathbf{x}_n$ containing the student's responses to a set of questions. $x_{i,j} = 1$ represents student $i$ has answered question $j$ correctly. Groups can be defined as the topic associated with each question. $\mathcal{I}_m$ contains the question IDs that belong to the same topic, and $\boldsymbol{\chi}_m$ represents a group of responses related to that topic. Clearly, not all students can answer every question. Thus, $\mathbf{X}_O$, $\mathbf{X}_U$ represent the existing responses and un-answered questions, respectively. The goal of VISL is to (i) predict students' responses to un-answered questions, which by itself is important in the education domain [56, 57], and (ii) discover the relationships between topics, which can help education experts optimize the learning experience and the curriculum. For structure learning, we adopt a Bayesian approach for graphs [18]. Namely, we seek to maximize the posterior probability of $\mathbf{G}$ given partially observed training data $\mathbf{X}_O$ within the space of all DAGs:

$$\mathbf{G}_\star = \arg\max\nolimits_{\mathbf{G}\in\text{DAGs}} \mathrm{p}(\mathbf{X}_O|\mathbf{G})\mathrm{p}(\mathbf{G}). \tag{1}$$

To optimize over the structure with the DAG constraint in Eq. 1, we resort to recent continuous optimization techniques [25, 63, 64], where a differentiable measure of 'DAG-ness', $\mathcal{R}(\mathbf{G}) = \mathrm{tr}(e^{\mathbf{G}\odot\mathbf{G}}) - D - 1$, was proposed and is zero if and only if $\mathbf{G}$ is a DAG. To leverage this DAG-ness characterisation, we follow Kyono et al. [25], Yu et al. [61] and introduce a regulariser based on $\mathcal{R}(\mathbf{G})$ to favour the DAG-ness of the solution, i.e.

$$\mathbf{G}_\star = \arg\max\nolimits_{\mathbf{G}} \left(\mathrm{p}(\mathbf{X}_O|\mathbf{G})\mathrm{p}(\mathbf{G}) - \lambda\mathcal{R}(\mathbf{G})\right). \tag{2}$$

In the following two sections, we present our detailed formulation, training and imputation algorithms of VISL, that allows the model to infer the latent structure $\mathbf{G}$ and impute missing values $\tilde{\mathbf{x}}_U$ in a test sample $\tilde{\mathbf{x}} \in \mathbb{R}^D$ based on the observed $\tilde{\mathbf{x}}_O$.

### 2.2 Generative model and variational inference

**Algorithm 1** Generative process

```
$\mathbf{G}_{ij} \sim$ Bernoulli$(p_{ij})$
for $n \in \{1, 2, \cdots, N\}$ do
    $\mathbf{Z}_n \sim \mathcal{N}(\mathbf{0}, \sigma_z^2\mathbf{I})$
    $\mathbf{x}_n \sim \mathcal{N}(f_\theta(\mathbf{Z}_n, \mathbf{G}), \sigma_x^2\mathbf{I})$
end for
```

For the generation of observation $\mathbf{X}$, we adopt the latent variable model of Fig. 1. Particularly, given an inferred graph $G$ and latent $\mathbf{Z}$, the generative path from $\mathbf{Z}$ to $\mathbf{X}$ is provided in Fig. 1, where we use a graph neural network (GNN) decoder that respects the learned graph structure $G$ and the provided grouping structure. Then the joint model likelihood is

$$\mathrm{p}\left(\mathbf{X}, \mathbf{Z}, \mathbf{G}\right) = \mathrm{p}(\mathbf{G}) \prod\nolimits_n \mathrm{p}(\mathbf{x}_n|\mathbf{Z}_n, \mathbf{G})\mathrm{p}(\mathbf{Z}_n). \tag{3}$$

Using this marginal likelihood $p(\mathbf{X})$ is consistent with Bayesian score based causal discovery [18]. As Kaiser and Sipos [22] and Reisach et al. [39] pointed out that other commonly used objectives, e.g. L2 loss in NOTEARS [63], are sensitive to data scaling and result in learning directions towards the high variance nodes. Loh and Bühlmann [28] and Ng et al. [35] showed that using a proper likelihood function can address these problems. Next, we leverage amortized variational inference to sidestep the intractable marginalization of the joint likelihood.

**Amortized variational inference.** The true posterior distribution over $\mathbf{Z}$ and $\mathbf{G}$ in Eq. 3 is intractable since we use a complex deep learning architecture. Therefore, we resort to an efficient amortized variational inference as in Kingma and Welling [24], Kingma et al. [23]. Here, we consider a fully factorized variational distribution $\mathrm{q}(\mathbf{Z}, \mathbf{G}|\mathbf{X}) = \mathrm{q}_\phi(\mathbf{G}) \prod_{n=1}^{N} \mathrm{q}_\phi(\mathbf{Z}_n|\mathbf{x}_n)$, where $\mathrm{q}_\phi(\mathbf{Z}_n|\mathbf{x}_n)$ is a Gaussian whose mean and (diagonal) covariance matrix are given by an *encoder*. For $\mathrm{q}(\mathbf{G})$, we consider the product of independent Bernoulli distributions over the edges; that is, the presence of each edge from $i$ to $j$ is associated with a probability $p_{ij}$ to be estimated. With the above formulation, the evidence lower bound (ELBO) is

$$\begin{aligned} \text{ELBO} = \textstyle\sum_n \big\{ &\mathbb{E}_{\mathrm{q}_\phi(\mathbf{Z}_n|\mathbf{x}_n)\mathrm{q}(\mathbf{G})}[\log \mathrm{p}(\mathbf{x}_n|\mathbf{Z}_n, \mathbf{G}) - \\ &\mathrm{KL}[\mathrm{q}_\phi(\mathbf{Z}_n|\mathbf{x}_n)||\mathrm{p}(\mathbf{Z}_n)]]\big\} - \mathrm{KL}[\mathrm{q}(\mathbf{G})||\mathrm{p}(\mathbf{G}))]. \end{aligned} \tag{4}$$

Next, we explain our choice of the generator (decoder), which uses a GNN over a learned graph $\mathbf{G}$ to model the interactions between latent variables, representing the information about each group. Then, we focus on the inference network (encoder), representing the mapping from the group of observed variables to its corresponding latent representation.

**Generator**. The generator (i.e., decoder) takes $\mathbf{Z}_n$ and $\mathbf{G}$ as inputs and outputs the reconstructed $\hat{\mathbf{x}}_n = f_\theta(\mathbf{Z}_n, \mathbf{G})$, where $\theta$ are the decoder parameters. In order to respect the pre-defined group structure, as shown in Fig. 1, $\mathbf{Z}_n$ is partitioned into $M$ parts, where $\mathbf{z}_{n,m}$ represents the latent variable for the group of observations $\boldsymbol{\chi}_{n,m}$. This defines a group-wise structured latent space. We adopt a two-step process for the generative path $\mathbf{Z}_n$ to $\mathbf{X}_n$: (i) GNN message passing with respect to the learned graph $\mathbf{G}$ between latent $\mathbf{z}_{n,m}$; (ii) final read-out layer to generate $\mathbf{X}_n$.

**GNN message passing in the generator**. In message passing, the information flows between nodes in $T$ consecutive node-to-edge (n2e) and edge-to-node (e2n) operations [13]. At the $t$-th step, we compute an embedding $\mathbf{h}^f_{i\to j}$ for each edge $i \to j$, called *forward* embedding, which summarizes the information sent from node $i$ to $j$. Specifically, the n2e/e2n operations in VISL are

$$\text{n2e}: \quad \mathbf{h}_{i\to j}^{(t),f} = \text{MLP}^f\left(\left[\mathbf{z}_i^{(t-1)}, \mathbf{z}_j^{(t-1)}\right]\right), \tag{5}$$

$$\text{e2n}: \quad \mathbf{z}_i^{(t)} = \text{MLP}^{e2n}\left(\textstyle\sum_{k\neq i} \mathbf{G}_{ki} \cdot \mathbf{h}_{k\to i}^{(t),f}\right). \tag{6}$$

Here, $t$ refers to the $t$-th iteration of message passing (that is, $\mathbf{Z}^{(0)} = \mathbf{Z}_n$, notice that we omit subindex $n$ for clarity). Finally, $\text{MLP}^f$, and $\text{MLP}^{e2n}$ are MLPs to be trained.

Interestingly, the message passing updates indicate that the information flows between latent nodes if a directed edge is specified in graph $\mathbf{G}$. Hence, the inferred structure $\mathbf{G}$ directly defines relations for latent space $\mathbf{Z}$ which contains the information of pre-defined groups. We show that under certain conditions, the inferred graph $G$ also represents the group-wise structure in observational space, and the corresponding model can be reformulated to a general *structural equation model* (SEM) [37] (see Appx. B).

**Read-out layer in the generator**. After $T$ iterations of GNN message passing, we have $\mathbf{Z}^{(T)}$. Due to we allow $\mathbf{Z}^{(T)}$ and $\mathbf{x}$ to have different dimensions, we apply a final function that maps $\mathbf{Z}^{(T)}$ to the reconstructed $\hat{\mathbf{x}}$, which also respects the pre-defined group structure. Since the observation $\mathbf{x} = [\boldsymbol{\chi}_1, \ldots, \boldsymbol{\chi}_M]$ may contain $\boldsymbol{\chi}_m$ with different dimensions, we adopt $M$ different MLPs, one for each group as the final read-out layer, to respect the group structure. Namely, $\hat{\mathbf{x}} = (g^1(\mathbf{z}_1^T), \ldots, g^M(\mathbf{z}_M^T))^\top$, where $g^m$ represents the MLP for group $m$. Thus, the decoder parameters $\boldsymbol{\theta}$ include the parameters of the following neural networks: MLP$^f$, MLP$^{e2n}$ and $g^m$ for $m = 1, \ldots, M$.

**Inference network**. As in standard VAEs, the encoder maps a sample $\mathbf{x}_n$ to its latent representation $\mathbf{Z}_n$. As discussed before, $\mathbf{Z}_n$ is partitioned into $M$ parts, where each $\mathbf{z}_{n,m}$ contains the information of the observation in group $m$. Similar to the read-out layer, we utilize the $M$ MLPs to map groups of observations to the mean/variance of the latent variables:

$$\begin{aligned}\boldsymbol{\mu}_n &= \left(\mu^1_{\phi_{\mu_1}}(\boldsymbol{\chi}_{n,1}), \ldots, \mu^M_{\phi_{\mu_M}}(\boldsymbol{\chi}_{n,M})\right)^\intercal, \\ \boldsymbol{\sigma}_n &= \left(\sigma^1_{\phi_{\sigma_1}}(\boldsymbol{\chi}_{n,1}), \ldots, \sigma^M_{\phi_{\sigma_M}}(\boldsymbol{\chi}_{n,M})\right)^\intercal.\end{aligned} \tag{7}$$

Here, $\mu^m_{\phi_{\mu_m}}$ and $\sigma^m_{\phi_{\sigma_m}}$ are neural networks for group $m$. When missing values are present, we replace them with a constant as in [34]. Under this formulation, VISL can infer latent variables $\mathbf{Z}_n$ from incomplete $\mathbf{x}_n$ for both training and test data. A graphic representation of how the encoder respects the structure of the latent space is shown in the appendix, Fig. 6(b).

### 2.3 Training VISL

Given the model described above, we propose the training objective to minimize w.r.t. $\theta$, $\phi$ and $\mathbf{G}$:

$$\mathcal{L}_{\text{VISL}}(\theta, \phi, \mathbf{G}) = -\text{ELBO} + \lambda\mathbb{E}_{\text{q}(\mathbf{G})}\left[\mathcal{R}(\mathbf{G})\right], \tag{8}$$

where ELBO is given by Eq. 4 and the DAG regulariser $\mathcal{R}(\mathbf{G})$ was introduced in Eq. 2 to favor the DAG-ness of learned graph $\mathbf{G}$.

**Evaluating the training loss $\mathcal{L}_{\textbf{VISL}}$**. VISL can work with any type of data. The log-likelihood term ($\log p_\theta(\mathbf{x}_n|\mathbf{Z}_n, \mathbf{G})$ in Eq. 4) is defined according to the data type. We use a Gaussian likelihood for continuous variables and a Bernoulli likelihood for binary ones. For the inference of $\mathbf{Z}$ and $\mathbf{G}$, the standard reparametrization trick is used to sample $\mathbf{Z}_n$ from the Gaussian $\text{q}_\phi(\mathbf{Z}_n|\mathbf{x}_n)$ [23, 24]. To backpropagate the gradients through the discrete variable $\mathbf{G}$, we resort to the Gumbel-softmax trick to sample from $\text{q}(\mathbf{G})$ [21, 31]. The $\text{KL}[\text{q}_\phi(\mathbf{Z}_n|\mathbf{x}_n)||\text{p}(\mathbf{Z}_n)]$ and $\text{KL}[\text{q}(\mathbf{G})||\text{p}(\mathbf{G})]$ terms can be obtained in closed-form since they are Gaussian distributions and independent Bernoulli distributions over the edges, respectively. This formulation brings additional advantages in real-life applications since one can easily incorporate domain knowledge and prior information into the VISL framework. For example, if the existence of a specific edge is known a priori, the edge probability can be set to 0/1 in the prior distribution. Finally, the DAG-loss regulariser in Eq. 8 can be computed by evaluating the function $\mathcal{R}$ on a Gumbel-softmax sample from $\text{q}(\mathbf{G})$. To adapt the model to different missing levels in the training data $\mathbf{X}$, we adopt the *masking* strategy [15, 30], which drops a random percent

**Algorithm 2** Training VISL.

```
Input  : Training dataset $\mathbf{X}$, possibly with missing values.
for each batch of samples $\{\mathbf{x}_n\}_{n \in B}$ do
    Drop a percentage of the data for each sample $\mathbf{x}_n$.
    Encode $\mathbf{x}_n$ through the reparametrization trick to sample $\mathbf{Z}_n \sim \mathcal{N}(\boldsymbol{\mu}_\phi(\mathbf{x}_n), \boldsymbol{\sigma}_\phi^2(\mathbf{x}_n))$ using Eq.7.
    Use the Gumbel-softmax to sample $\mathbf{G}$ from $\mathrm{q}(\mathbf{G})$.
    Use decoder to reconstruct $\hat{\mathbf{x}}_n = f_\theta(\mathbf{Z}_n, \mathbf{G})$.
    Calculate the training loss $\mathcal{L}_{\text{VISL}}$ (Eq. 8).
    Gradient step w.r.t. $\phi$ (encoder parameters), $\theta$ (decoder parameters) and $\mathbf{G}$ (posterior edge probabilities).
Output : Encoder parameters $\phi$, decoder parameters $\theta$, and posterior probabilities over the edges $\mathbf{G}$.
```

of the observed values during training. The entire training procedure for VISL is summarised in Algorithm 2.

**Two-step training**. After training, we obtain the posterior of the graph $\mathbf{G}$, which respects the underlying structure of the groups as shown in Appx. B. With the trained network, we can impute missing values in the groups where their ancestors contain some observations but if a group has no ancestors no information can be propagated during imputation. After learning the graph structure and to facilitate the imputation task, we introduce a *backwards* edge: for an edge from $j$ to $i$ we denote the backwards edge information as $\mathbf{h}^b_{i\to j}$ which codifies the information that the $i \to j$ edge lets flow from the $j$-th to the $i$-th node. It is defined in the same way as Eq. 5, i.e.,: $\mathbf{h}^{(t),b}_{i\to j} = \mathrm{MLP}^b\left(\left[\mathbf{z}_i^{(t-1)}, \mathbf{z}_j^{(t-1)}\right]\right)$, where $\mathrm{MLP}^b$ is the backward MLP; and the e2n update (Eq.6) is modified to $\mathbf{z}_i^{(t)} = \mathrm{MLP}^{e2n}\left(\sum_{k\neq i} \mathbf{G}_{ki} \cdot \left\{\mathbf{h}^{(t),f}_{k\to i} + \mathbf{h}^{(t),b}_{i\to k}\right\}\right)$.

In summary, we propose a two-stage training process, where the first stage — described in previous sections — focuses on discovering the edge directions between nodes without the $\mathrm{MLP}^b$ (i.e., we do not train the $\mathrm{MLP}^b$). In the second stage, we fix the graph structure $\mathbf{G}$ and continue to train the model with the backward MLP. This two-stage training process allows VISL to leverage the backward MLP for the imputation task without updating the graph structure.

**Revisiting the learning objectives**. The optimal graph of relationships, denoted as $\mathbf{G}_\star$ in Eq. 2, is given by the estimated posterior probabilities of graph $\mathbf{G}$. In addition, the regularizer $\mathcal{R}(\mathbf{G})$ provides a way to evaluate if the resulting graph is a DAG. By tuning the regularizer strength $\lambda$, one can ensure that the resulting $\mathbf{G}^*$ represents a proper DAG.

For imputation, similar to Ma et al. [30], Nazabal et al. [34], the trained model can impute missing values for a test instance $\widetilde{\mathbf{x}}$ as

$$\mathrm{p}(\widetilde{\mathbf{x}}_U | \widetilde{\mathbf{x}}_O, \mathbf{X}) = \mathbb{E}_{\mathrm{q}_\phi(\mathbf{Z}|\widetilde{\mathbf{x}})\mathrm{q}(\mathbf{G})} \mathrm{p}(\widetilde{\mathbf{x}}_U | \mathbf{Z}, \mathbf{G}). \tag{9}$$

Therefore, the distribution over $\widetilde{\mathbf{x}}_U$ (missing values) is obtained by applying the encoder and decoder with $\widetilde{\mathbf{x}}$ as input. Previous work [30, 34] also uses variational autoencoders for missing value imputation, which can have problems with overfitting due to spurious correlations [25] even with sufficient training data. One important distinction of VISL is the incorporation of the learned structure $\mathbf{G}$, which helps the model to be robust to spurious correlations.

**Special case: variable-wise relations**. In the above formulation, we have defined VISL for group-wise structure learning. Variable-wise relations can be regarded as a special case. In particular, we can set $M = D$ and $\mathcal{I}_m = \{m\}$ (see Fig. 5 (a) in the appendix), i.e. each group only contains a single variable. Through this modification, we can further simplify the encoder and read-out layer. Instead of using $M$ different MLPs, a single MLP can be shared across all variables since each group has dimension of 1. The mean function for the encoder is then defined as

$$\boldsymbol{\mu}_n = \left(\mu_\phi(x_{n,1}), \ldots, \mu_\phi(x_{n,D})\right). \tag{10}$$

One can define encoder variance $\boldsymbol{\sigma}$ (Fig. 6 (a) in the appendix) and the read-out layer $g$ analogously.

**Computational cost.** The main computational bottleneck is the training of VISL, where we require a different inference network and read-out layer for each group $m \in M$. However, some weight sharing schemes can be used to reduce the computational cost. When each group has the same dimensionality, we share the weights of the inference networks. In the case of different dimensionalities, one can infer the latent variables by parallelizing inference network forward passes to reduce computational cost. Table 11 in appendix provides the wall-clock time comparison for each of the methods for up to 512 variables. We can see that all deep learning based methods (i.e. NOTEARS, DAG-GNN, VISL, etc.) have similar time complexity.

## 3 Related Work

Since VISL simultaneously tackles missing value imputation and structure learning, we review both fields. Moreover, we review recent works regarding improving the deep learning performance with structure learning. Finally, as one of the focused applications of this work is education, we review recent advances of AI in education.

**Structure learning**. Structure learning aims to infer the underlying structures associated with some observations. There are mainly three types of methods: constrained-based, score-based, and hybrid. Constraint-based ones exploit (conditional) independence tests to find the underlying structure, such as PC [47] and Fast Causal Inference (FCI) [48]. They have recently been extended to handle partially observed data through test-wise deletion and adjustments [50, 52]. Score-based methods find the structure by optimizing a proper scoring function. The core difficulty lies in the number of possible graphs growing super-exponentially with the number of nodes [4]. Thus, explicitly solving the optimization can only be done up to a few nodes [7, 36, 46]. Therefore, approximation have been proposed to ease the computational burden, including searching over topological ordering [43, 44, 51], greedy search [3, 38], coordinate descent [1, 11, 17].

Recently, continuous optimization, called *Notears*, has become very popular [63]. *Notears* proposed a differentiable characterization of the DAG to learn the model parameters and graph structures jointly. *Notears* has inspired the development of other methods, *Notears-MLP* and *Notears-Sob* [64], *Grandag* [26], and *DAG-GNN* [61], which extends to model nonlinear relationships between variables. However, their formulations cannot handle missing values and have been observed to be sensitive to data scaling [22]. *DAG-GNN* also adopts a specially-designed GNN to perform structure learning [61]. There are three key distinctions compared to VISL: (i) our model handles the group-wise relationship, while DAG-GNN focuses on variables level; (ii) our model is capable of missing value imputation and group-wise structure learning simultaneously, whereas the original formulation of DAG-GNN and related work require complete data; (iii) VISL adopts Bayesian view for the graphs, compared to a point estimation. VISL is also related to Bayesian DAG learning. Viinikka et al. [55] proposed to sample the graph posterior using MCMC, but it suffers from high computation complexity. VISL, in contrary, can easily be scaled to high dimensional datasets. BCD [6] and DiBS [29] have recently leveraged the approximate inference for scalable Bayesian DAG learning. BCD nets focused on linear Gaussian SEM (v.s. nonlinear relationship by VISL). DiBS adopted a full Bayesian treatment and used a particle sampler to draw from a joint posterior. Compared to VISL, it cannot handle missing values nor variable groups. Geffner et al. [12] recently proposed an end-to-end causal inference framework (DECI) combining causal discovery and inference with missing data. Compared to VISL, DECI is built upon nonlinear additive noise models [19], whereas VISL uses an autoencoder structure with a GNN decoder. When the GNN reaches equilibrium state, Appendix B shows that VISL represents a general SEM, which includes additive noise models as a special case. Apart from the likelihood-based causal discovery, Rolland et al. [40] used score matching to extract causal relationships for non-linear additive noise models. Our work differs in four aspects: (1) structure learning (VISL) v.s. causal discovery; (2) VISL is based on the auto-encoder framework; (3) VISL can handle MAR missing data and (4) VISL uses a Bayesian view of graphs.

**Structure deep learning**. Continuous optimization for learning structures has been used to boost performance in classification. In CASTLE [25], structure learning is introduced as a regulariser for a classification model. This regulariser reconstructs only the most relevant features, leading to improved out-of-sample predictions. In SLAPS [10], the classification objective is supplemented with a self-supervised task that learns a graph of interactions between variables through a GNN. These works focused on leveraging the structure learning instead of advancing its performance.

**Missing values imputation**. The relevance of missing data in real-world problems has motivated a long history of research [9, 41]. A popular approach is to estimate the missing values based on the observed ones through different techniques [45], e.g. Random Forest [49], Bayesian Ridge Regression [2]. Wu et al. [59] explored the use of generative model for missing value imputation, although fully observed training data is required. This limitation is addressed in both Nazabal et al. [34] with zero-imputing strategy, and Ma et al. [30] with a permutation invariant set encoder. Mattei and Frellsen [32] proposed to use the importance weighted autoencoder, which enables a tighter lower bound than ELBO and leads to improved performance. Ivanov et al. [20] parameterized the imputation as sampling from a conditional distribution, and proposed a method for arbitrary conditioning with VAEs.

**AI in education**. There has been tremendous progress in AI for educational applications, e.g. knowledge tracing [27, 33, 54]; grading students' performance [58]; generating feedback for students working on coding challenges [60]. In particular, most related to VISL is imputing missing values in students' responses. Wang et al. [56] adopts a partial VAE [30] to perform missing value imputation and personalization. However, partial VAE does not consider the structural relations between questions/topics. With the additional insights from structure learning, VISL can provide more information to teachers to help curriculum design than just imputations.

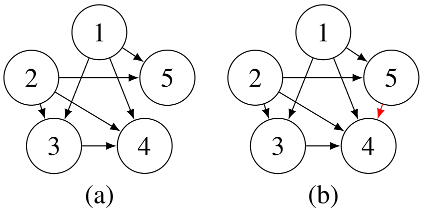

Figure 2: (a): Structure simulated for one of the synthetic datasets with 5 variables. (b): Graph predicted by VISL (when the one on the left is used as the true one). VISL recovers the ground truth graph with one addition edge from 5 to 4.

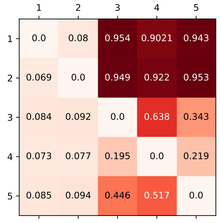

Figure 3: Probability of edges obtained by VISL in the synthetic experiment. By using a 0.5 threshold, we get the predicted graph in Fig. 2(b). Item $(i, j)$ refers to the probability of edge $i \rightarrow j$.

| | RMSE |
|---|---|
| Major | 0.54±0.0032 |
| Mean | 0.22±0.0061 |
| MICE | 0.14±0.0046 |
| Missforest | 0.13±0.0025 |
| PVAE | 0.14±0.0043 |
| VISL | **0.12±0.004** |

Table 1: Imputation results for the synthetic experiment. Mean and standard error over 15 datasets.

| | Adjacency | | | Orientation | | | Causal accuracy |
|---|---|---|---|---|---|---|---|
| | Recall | Precision | $F_1$-score | Recall | Precision | $F_1$-score | |
| PC | 0.42±0.056 | 0.63±0.067 | 0.49±0.056 | 0.22±0.046 | 0.33±0.061 | 0.26±0.051 | 0.33±0.046 |
| GES | 0.45±0.044 | 0.57±0.036 | 0.49±0.038 | 0.25±0.046 | 0.31±0.053 | 0.27±0.049 | 0.36±0.045 |
| NOT. (L) | 0.19±0.028 | 0.44±0.059 | 0.27±0.036 | 0.15±0.023 | 0.37±0.060 | 0.21±0.032 | 0.15±0.023 |
| NOT. (NL) | 0.33±0.039 | 0.49±0.051 | 0.39±0.044 | 0.28±0.032 | 0.42±0.043 | 0.33±0.035 | 0.28±0.032 |
| DAG-GNN | 0.44±0.064 | 0.51±0.062 | 0.46±0.061 | 0.35±0.050 | 0.42±0.052 | 0.37±0.049 | 0.35±0.050 |
| VISL | **0.78±0.084** | **0.73±0.078** | **0.74±0.063** | **0.66±0.13** | **0.60±0.10** | **0.63±0.10** | **0.66±0.13** |

Table 2: Structure discovery results for synthetic experiment (mean and std error over 15 datasets).

## 4 Experiments

We evaluate the performance of VISL in three different problems: a synthetic experiment where the data generation process is controlled, a semi-synthetic problem (simulated data from a real-world problem) (Neuropathic Pain), and the real-world problem that motivated the group-level structure learning (Eedi). The first two datasets are on the variable level. The last one focuses on the group level and real-world usage, and have worked closely with the domain expert to evaluate the results. Additional experiments are presented in the appendix.

**Baselines**. We consider five baselines for the structure discovery task at the variable level. PC [48] and GES [3] are popular constraint-based and score-based approaches, respectively. NOTEARS (NOT.) [63], the non-linear (NL) extension of NOTEARS [64], and DAG-GNN [61] are the other three closely related baselines. Unlike VISL, these baselines cannot deal with missing values. Therefore, we work with complete training data in the first two sections. The Eedi real-world data is only partially observed, where these baselines are not applicable. For the missing data imputation, we also consider five baselines. Mean Imputing (Mean), Majority Vote (Major) (refer to Appx. D for short descriptions), Missforest [49] and MICE [2] are four widely-used imputation algorithms, and PVAE [30] is a recent algorithm based on amortized inference.

| | Accuracy | AUROC | AUPR |
|---|---|---|---|
| Major | 0.9268±0.0003 | 0.5304±0.0003 | 0.3366±0.0025 |
| Mean | 0.9268±0.0003 | 0.8529±0.0012 | 0.3262±0.0034 |
| MICE | 0.9469±0.0007 | 0.9319±0.0010 | 0.6513±0.0046 |
| Missforest | 0.9305±0.0004 | 0.8915±0.0093 | 0.5227±0.0033 |
| PVAE | 0.9415±0.0003 | 0.9270±0.0007 | 0.5934±0.0046 |
| VISL | **0.9471±0.0006** | **0.9392±0.0008** | **0.6597±0.0053** |

Table 3: Imputation results for neuropathic pain data (mean and std error over five runs).

| | Adjacency | | | Orientation | | | Causal Accuracy |
|---|---|---|---|---|---|---|---|
| | Recall | Precision | $F_1$-score | Recall | Precision | $F_1$-score | |
| PC | 0.046±0.001 | 0.375±0.006 | 0.082±0.001 | 0.024±0.001 | 0.199±0.011 | 0.044±0.002 | 0.058±0.003 |
| GES | 0.110±0.001 | 0.436±0.008 | 0.176±0.002 | 0.082±0.001 | 0.323±0.009 | 0.131±0.003 | 0.121±0.001 |
| NOT. (L) | 0.006±0.000 | 0.011±0.001 | 0.008±0.000 | 0.001±0.000 | 0.001±0.001 | 0.001±0.000 | 0.001±0.000 |
| NOT. (NL) | 0.011±0.001 | **0.644±0.025** | 0.022±0.002 | 0.006±0.001 | 0.354±0.018 | 0.012±0.001 | 0.006±0.001 |
| DAG-GNN | 0.129±0.028 | 0.272±0.101 | 0.128±0.027 | 0.051±0.010 | 0.126±0.059 | 0.050±0.007 | 0.051±0.010 |
| VISL | **0.261±0.006** | 0.637±0.009 | **0.370±0.005** | **0.236±0.007** | **0.573±0.005** | **0.334±0.006** | **0.245±0.006** |

Table 4: Structure discovery results for neuropathic pain data (mean and std error over five runs).

**Metrics**. Imputation performance is evaluated with standard metrics such as RMSE (continuous variables) and accuracy (binary variables). For binary variables , we also provide the area under the ROC and the Precision-Recall curves (AUROC and AUPR, respectively), which are especially useful for imbalanced data (such as Neuropathic Pain). We follow common practice [14, 52] regarding structure discovery performance, and consider metrics on the *adjacency* and *orientation*. While the former does not take into account the direction of the edges, the latter does. We report recall, precision and $F_1$-score. We also provide *causal accuracy*, a discovery metric that considers orientation [5].

### 4.1 Synthetic experiment

We simulate fifteen synthetic datasets. For each simulated dataset, we first sample the true structure $\mathbf{G}$; see Fig. 2(a) for an example. The appendix provides detailed generation mechanism, including a visualisation of the data in Fig. 7. For each dataset, we simulate 5000 training and 1000 test samples.

**Imputation performance**. VISL outperforms the baselines in terms of imputation across all synthetic datasets ( Table 1).The results grouped by the number of variables are presented by Table 8 in the appendix.

**Structure discovery performance**. VISL obtains better performance than the baselines, see Table 2. The results split by the number of variables are shown in the appendix, Table 10. Specifically, we observe VISL consistently outperforms the baseline method in all metrics considered with all datasets (see Table 10). In this small synthetic experiment, it is possible to visualize the predicted graph. Fig. 3 shows the posterior probability of each edge (i.e. the estimated matrix $\mathbf{G}$) for the simulated dataset in Fig. 2(a). Using a threshold of 0.5, we obtain the predicted graph in Fig. 2(b). We observed that VISL recovers the ground truth graphs with one additional edge. The sources of its advanced performances are twofold: 1) VISL uses the ELBO (Eq. 4) as training objective, a surrogate for marginal likelihood. Kaiser and Sipos [22], Reisach et al. [39] reported that L2 loss used in NOTEARS is sensitive to data scaling and directs the learning of directions towards high variance nodes. This can be resolved by using a proper likelihood training objective [28, 35]; 2) instead of using observed variables to construct the structural equation model (NOTEARS) or designing a specialized GNN structure (DAG-GNN), VISL is more flexible in terms of transforming the observed variables into a latent distribution via the encoder, and adopting a general message-passing GNN decoder.

Finally, VISL can scale to large data in terms of data points and dimensionality. We demonstrate the computational efficiency with synthetic data ranging from 4 to 512 nodes in the appendix, Table 11.

### 4.2 Neuropathic pain dataset

We evaluate our method using a benchmark in healthcare applications [53]. The dataset contains records of patients regarding the symptoms associated with neuropathic pain. There are 222 variables

|  | Accuracy | AUROC | AUPR |
|---|---|---|---|
| Major | 0.6260±0.0000 | 0.6208±0.0000 | 0.7465±0.0000 |
| Mean | 0.6260±0.0000 | 0.6753±0.0000 | 0.6906±0.0000 |
| MICE | 0.6794±0.0005 | 0.7453±0.0007 | 0.7483±0.0010 |
| Missforest | 0.6849±0.0005 | 0.7219±0.0007 | 0.7478±0.0008 |
| PVAE | 0.7138±0.0005 | **0.7852±0.0001** | **0.8204±0.0002** |
| VISL | **0.7147±0.0007** | 0.7815±0.0008 | 0.8179±0.0006 |

Table 5: Imputation results for Eedi topics dataset (mean and standard error over five runs).

|  | Adjacency |  | Orientation |  |
|---|---|---|---|---|
|  | Expt 1 | Expt 2 | Expt 1 | Expt 2 |
| *Random* | 2.04 | 2.08 | 1.44 | 1.40 |
| DAG-GNN | 2.04 | 2.32 | 1.68 | 1.68 |
| VISL | **3.60** | **3.70** | **2.76** | **2.60** |

Table 6: Average expert evaluation of the topic relationships. Cohen's $\kappa$ inter-annotator agreement is $0.72$ for adjacency and $0.76$ for orientation (substantial agreement).

in this dataset. Unlike the previous experiment with continuous data, this dataset has binary variables indicating the symptoms. The train and test sets have $1000$ and $500$ patients, respectively.

**Imputation performance**. VISL shows competitive or superior performance when compared to the baselines, see Table 3. Notice that AUROC and AUPR allow for an appropriate threshold-free assessment in this imbalanced scenario. Indeed, as expected from medical data, the minority of values are 1 (symptoms); here, the prevalence of symptoms is around $8\%$ in the test set. Interestingly, it is precisely in AUPR where the differences between VISL and the rest of the baselines are larger except MICE, whose performance is very similar to VISL in this dataset.

**Structure discovery results**. As in the synthetic experiment, VISL outperforms the causality-based baselines; see Table 4. Notice that NOTEARS (NL) is slightly better in terms of adjacency-precision, i.e. the edges that it predicts are slightly more reliable. However, this is at the expense of a significantly lower capacity to detect true edges, see the recall and the trade-off between both ($\mathrm{F}_1$-score).

### 4.3 Eedi topics dataset

Finally, we evaluate our method on an even more challenging real-world dataset in education to discover the group-wise structure between topics while the observations are question-answer pairs under these topics. This is an important real-world problem in the field of AI-powered educational systems [56, 57]. This dataset is very sparse, with 74.1% of the values missing. The dataset contains the responses from 6147 students to 948 mathematics questions. The 948 variables are binary (1: correct and 0 otherwise). These questions target specific mathematical concepts and are grouped into a meaningful hierarchy of *topics*; see Fig. 4 in Appx. E. Here we apply VISL to find the structures among the topics using the third level hierarchy (Fig. 4), resulting in 57 group-level nodes.

**Imputation results.** VISL achieves competitive or superior performance when compared to the baselines (Table 5). Although the dataset is more balanced (54% of the values are 1), we provide AUROC and AUPR for completeness. Notice that this setting is more challenging since the information flows at less granular level (i.e. group). Interestingly, even in this case, VISL obtains similar or improved imputation results compared to the baselines.

**Structure discovery results between groups.** Most of the baselines used so far cannot be applied here because i) they cannot deal with missing data or ii) they cannot learn group-level relationships. DAG-GNN is the only one that can be adapted to satisfy both properties. For missing data, we adapt DAG-GNN following the same strategy as in VISL, i.e. replacing missing entries with a constant value. For the second one, we further adapt it by using group-specific mappings like VISL to cope with arbitrary groups. We also include another baseline, *Random*, where the structures between topics are randomly sampled from a Bernoulli distribution. Due to the lack of ground truth relationships, we ask two experts (teachers) to assess the validity of the relationships found by VISL, DAG-GNN, and *Random*. For each relationship, they are asked to rate a value from 1 (strongly disagree) to 5 (strongly agree) for the adjacency (whether it is sensible to connect the two topics) and the orientation (whether the first one is a prerequisite for the second one). We release the the complete list of relationships and expert evaluations for VISL, DAG-GNN, and *Random*; see Table 15, Table 16, and Table 17, respectively. Thus, the results is reproducible and allow the community to build on this data as a structure discovery benchmark. In summary, Table 6 shows here the average evaluations: we see that the relationships discovered by VISL score much more highly across both metrics than the baseline models.

Another interesting aspect is how the relationships between level-3 topics are distributed in higher-level topics. Intuitively, it is expected that most of the relationships happen *inside* higher-level topics (e.g. Number-related concepts are more probably related to each other than to Geometry-related ones). Table 7 in appendix shows the distribution for the compared methods. Indeed, notice that the percentage of inside-topic relationships is higher for VISL (82%) and DAG-GNN (42%) than for *Random* (34%). An analogous analysis for the 25 level-2 topics is provided in the appendix; see Table 12 (VISL), Table 13 (DAG-GNN), and Table 14 (*Random*). 6% of the connections happen inside level 2 topics for *Random*, it is 14% for DAG-GNN and 36% for VISL.

**Education Impact.** Lastly, to make a real-world impact, we have been provided with an additional education dataset in the same format as Eedi by an education organization to help provide insight for math curriculum building. The final structure among all topics found by VISL is presented by figure Fig. 8 in the appendix. This figure provides insights into which topics are foundational and need to be covered earlier (topics with many originating edges), or later (topics with many incoming edges). This allowed us to re-evaluate the order of topics in a nationwide used secondary curriculum. Specifically, topics such as “arithmetic” or “properties of shapes” were moved earlier in the curriculum, while topics such as “negative numbers” or “proportion and similarity” were moved to a later stage in the curriculum. Another interesting example found by the domain expert are “Venn diagrams”, which were originally taught in year 9/10 and are now suggested to be moved to year 7. Experts found that the topic “Venn diagram” has been a useful tool in teaching other topics which are currently taught before year 10. This emphasises the real-world impact our model can have in planning curricula.

## 5 Conclusions

We introduced VISL, a novel approach that simultaneously performs group-wise structure discovery and learns to impute missing values. Both tasks are performed jointly: imputation is informed by the discovered relationships and vice-versa, leading to improved performance for both tasks. Moreover, motivated by a real-world problem, VISLshows its impact in the real-world education domain to aid domain experts in setting up curriculum. Despite of the improved performance on structure learning with missing data, VISL can be further extended in several directions. First, one potential limitation is that the inferred structure from VISL is not causal. Appendix B shows that VISL satisfies the cauasl Markov assumption under equilibrium, which opens a door for potential causal claims. Another direction for future work is to extend the M(C)AR assumption to *missing not at random*(MNAR), which can be more practical for real world usage. In the end, the performance can further be boosted by designing better graph posteriors beyond an independent Bernoulli distribution.

## Acknowledgments and Disclosure of Funding

PMA acknowledges project PY20_00286 funded by Junta de Andalucía.

## References

[1] Bryon Aragam and Qing Zhou. Concave penalized estimation of sparse gaussian bayesian networks. *The Journal of Machine Learning Research*, 16(1):2273–2328, 2015.

[2] S van Buuren and Karin Groothuis-Oudshoorn. mice: Multivariate imputation by chained equations in r. *Journal of statistical software*, pages 1–68, 2010.

[3] David Maxwell Chickering. Optimal structure identification with greedy search. *Journal of machine learning research*, 3(Nov):507–554, 2002.

[4] Max Chickering, David Heckerman, and Chris Meek. Large-sample learning of bayesian networks is np-hard. *Journal of Machine Learning Research*, 5, 2004.

[5] Tom Claassen and Tom Heskes. A bayesian approach to constraint based causal inference. In *Proceedings of the Twenty-Eighth Conference on Uncertainty in Artificial Intelligence*, pages 207–216, 2012.

[6] Chris Cundy, Aditya Grover, and Stefano Ermon. Bcd nets: Scalable variational approaches for bayesian causal discovery. *Advances in Neural Information Processing Systems*, 34, 2021.

[7] James Cussens, David Haws, and Milan Studenỳ. Polyhedral aspects of score equivalence in bayesian network structure learning. *Mathematical Programming*, 164(1):285–324, 2017.

[8] Hanjun Dai, Zornitsa Kozareva, Bo Dai, Alex Smola, and Le Song. Learning steady-states of iterative algorithms over graphs. In *International conference on machine learning*, pages 1106–1114. PMLR, 2018.

[9] Arthur P Dempster, Nan M Laird, and Donald B Rubin. Maximum likelihood from incomplete data via the em algorithm. *Journal of the Royal Statistical Society: Series B (Methodological)*, 39(1):1–22, 1977.

[10] Bahare Fatemi, Layla El Asri, and Seyed Mehran Kazemi. Slaps: Self-supervision improves structure learning for graph neural networks. *arXiv preprint arXiv:2102.05034*, 2021.

[11] Fei Fu and Qing Zhou. Learning sparse causal gaussian networks with experimental intervention: regularization and coordinate descent. *Journal of the American Statistical Association*, 108 (501):288–300, 2013.

[12] Tomas Geffner, Javier Antoran, Adam Foster, Wenbo Gong, Chao Ma, Emre Kiciman, Amit Sharma, Angus Lamb, Martin Kukla, Nick Pawlowski, et al. Deep end-to-end causal inference. *arXiv preprint arXiv:2202.02195*, 2022.

[13] Justin Gilmer, Samuel S Schoenholz, Patrick F Riley, Oriol Vinyals, and George E Dahl. Neural message passing for quantum chemistry. In *International Conference on Machine Learning*, pages 1263–1272. PMLR, 2017.

[14] Clark Glymour, Kun Zhang, and Peter Spirtes. Review of causal discovery methods based on graphical models. *Frontiers in genetics*, 10:524, 2019.

[15] Wenbo Gong, Sebastian Tschiatschek, Richard Turner, Sebastian Nowozin, José Miguel Hernández-Lobato, and Cheng Zhang. Icebreaker: Element-wise active information acquisition with bayesian deep latent gaussian model. In *Advances in Neural Information Processing Systems*, 2019.

[16] Fangda Gu, Heng Chang, Wenwu Zhu, Somayeh Sojoudi, and Laurent El Ghaoui. Implicit graph neural networks. *arXiv preprint arXiv:2009.06211*, 2020.

[17] Jiaying Gu, Fei Fu, and Qing Zhou. Penalized estimation of directed acyclic graphs from discrete data. *Statistics and Computing*, 29(1):161–176, 2019.

[18] David Heckerman, Christopher Meek, and Gregory Cooper. A bayesian approach to causal discovery. In *Innovations in Machine Learning*, pages 1–28. Springer, 2006.

[19] Patrik Hoyer, Dominik Janzing, Joris M Mooij, Jonas Peters, and Bernhard Schölkopf. Nonlinear causal discovery with additive noise models. *Advances in neural information processing systems*, 21:689–696, 2008.

[20] Oleg Ivanov, Michael Figurnov, and Dmitry Vetrov. Variational autoencoder with arbitrary conditioning. *arXiv preprint arXiv:1806.02382*, 2018.

[21] Eric Jang, Shixiang Gu, and Ben Poole. Categorical reparameterization with gumbel-softmax. In *International conference on learning representations*, 2017.

[22] Marcus Kaiser and Maksim Sipos. Unsuitability of NOTEARS for causal graph discovery. *CoRR*, abs/2104.05441, 2021. URL https://arxiv.org/abs/2104.05441.

[23] Diederik P Kingma, Max Welling, et al. An introduction to variational autoencoders. *Foundations and Trends® in Machine Learning*, 12(4):307–392, 2019.

[24] D.P. Kingma and M. Welling. Auto-encoding variational bayes. *arXiv preprint arXiv:1312.6114*, 2013.

[25] Trent Kyono, Yao Zhang, and Mihaela van der Schaar. Castle: Regularization via auxiliary causal graph discovery. In H. Larochelle, M. Ranzato, R. Hadsell, M. F. Balcan, and H. Lin, editors, *Advances in Neural Information Processing Systems*, volume 33, pages 1501–1512. Curran Associates, Inc., 2020. URL https://proceedings.neurips.cc/paper/2020/file/1068bceb19323fe72b2b344ccf85c254-Paper.pdf.

[26] Sébastien Lachapelle, Philippe Brouillard, Tristan Deleu, and Simon Lacoste-Julien. Gradient-based neural dag learning. *arXiv preprint arXiv:1906.02226*, 2019.

[27] Andrew S Lan, Christoph Studer, and Richard G Baraniuk. Time-varying learning and content analytics via sparse factor analysis. In *Proceedings of the 20th ACM SIGKDD international conference on Knowledge discovery and data mining*, pages 452–461, 2014.

[28] Po-Ling Loh and Peter Bühlmann. High-dimensional learning of linear causal networks via inverse covariance estimation. *The Journal of Machine Learning Research*, 15(1):3065–3105, 2014.

[29] Lars Lorch, Jonas Rothfuss, Bernhard Schölkopf, and Andreas Krause. Dibs: Differentiable bayesian structure learning. *Advances in Neural Information Processing Systems*, 34, 2021.

[30] Chao Ma, Sebastian Tschiatschek, Konstantina Palla, Jose Miguel Hernandez-Lobato, Sebastian Nowozin, and Cheng Zhang. EDDI: Efficient dynamic discovery of high-value information with partial VAE. In Kamalika Chaudhuri and Ruslan Salakhutdinov, editors, *Proceedings of the 36th International Conference on Machine Learning*, volume 97 of *Proceedings of Machine Learning Research*, pages 4234–4243. PMLR, 09–15 Jun 2019. URL http://proceedings.mlr.press/v97/ma19c.html.

[31] Chris J Maddison, Andriy Mnih, and Yee Whye Teh. The concrete distribution: A continuous relaxation of discrete random variables. In *International conference on learning representations*, 2017.

[32] Pierre-Alexandre Mattei and Jes Frellsen. Miwae: Deep generative modelling and imputation of incomplete data sets. In *International conference on machine learning*, pages 4413–4423. PMLR, 2019.

[33] Junpei Naito, Yukino Baba, Hisashi Kashima, Takenori Takaki, and Takuya Funo. Predictive modeling of learning continuation in preschool education using temporal patterns of development tests. In *Proceedings of the AAAI Conference on Artificial Intelligence*, volume 32, 2018.

[34] Alfredo Nazabal, Pablo M Olmos, Zoubin Ghahramani, and Isabel Valera. Handling incomplete heterogeneous data using vaes. *Pattern Recognition*, 107:107501, 2020.

[35] Ignavier Ng, AmirEmad Ghassami, and Kun Zhang. On the role of sparsity and dag constraints for learning linear dags. *Advances in Neural Information Processing Systems*, 33:17943–17954, 2020.

[36] Sascha Ott and Satoru Miyano. Finding optimal gene networks using biological constraints. *Genome Informatics*, 14:124–133, 2003.

[37] Jonas Peters, Dominik Janzing, and Bernhard Schölkopf. *Elements of causal inference: foundations and learning algorithms*. The MIT Press, 2017.

[38] Joseph Ramsey, Madelyn Glymour, Ruben Sanchez-Romero, and Clark Glymour. A million variables and more: the fast greedy equivalence search algorithm for learning high-dimensional graphical causal models, with an application to functional magnetic resonance images. *International journal of data science and analytics*, 3(2):121–129, 2017.

[39] Alexander G Reisach, Christof Seiler, and Sebastian Weichwald. Beware of the simulated dag! varsortability in additive noise models. *arXiv preprint arXiv:2102.13647*, 2021.

[40] Paul Rolland, Volkan Cevher, Matthäus Kleindessner, Chris Russell, Dominik Janzing, Bernhard Schölkopf, and Francesco Locatello. Score matching enables causal discovery of nonlinear additive noise models. In *International Conference on Machine Learning*, pages 18741–18753. PMLR, 2022.

[41] Donald B Rubin. Inference and missing data. *Biometrika*, 63(3):581–592, 1976.

[42] Karen Sachs, Omar Perez, Dana Pe'er, Douglas A Lauffenburger, and Garry P Nolan. Causal protein-signaling networks derived from multiparameter single-cell data. *Science*, 308(5721): 523–529, 2005.

[43] Mauro Scanagatta, Cassio P de Campos, Giorgio Corani, and Marco Zaffalon. Learning bayesian networks with thousands of variables. In *NIPS*, pages 1864–1872, 2015.

[44] Mauro Scanagatta, Giorgio Corani, Cassio P De Campos, and Marco Zaffalon. Learning treewidth-bounded bayesian networks with thousands of variables. In *NIPS*, pages 1462–1470, 2016.

[45] Judi Scheffer. Dealing with missing data. In *Research Letters in the Information and Mathematical Sciences*, pages 153–160, 2002.

[46] Ajit P Singh and Andrew W Moore. *Finding optimal Bayesian networks by dynamic programming*. Citeseer, 2005.

[47] Peter Spirtes and Clark Glymour. An algorithm for fast recovery of sparse causal graphs. *Social science computer review*, 9(1):62–72, 1991.

[48] Peter Spirtes, Clark N Glymour, Richard Scheines, and David Heckerman. *Causation, prediction, and search*. MIT press, 2000.

[49] Daniel J Stekhoven and Peter Bühlmann. Missforest—non-parametric missing value imputation for mixed-type data. *Bioinformatics*, 28(1):112–118, 2012.

[50] Eric V Strobl, Shyam Visweswaran, and Peter L Spirtes. Fast causal inference with non-random missingness by test-wise deletion. *International journal of data science and analytics*, 6(1): 47–62, 2018.

[51] Marc Teyssier and Daphne Koller. Ordering-based search: A simple and effective algorithm for learning bayesian networks. *arXiv preprint arXiv:1207.1429*, 2012.

[52] Ruibo Tu, Cheng Zhang, Paul Ackermann, Karthika Mohan, Hedvig Kjellström, and Kun Zhang. Causal discovery in the presence of missing data. In *The 22nd International Conference on Artificial Intelligence and Statistics*, pages 1762–1770. PMLR, 2019.

[53] Ruibo Tu, Kun Zhang, Bo Christer Bertilson, Hedvig Kjellström, and Cheng Zhang. Neuropathic pain diagnosis simulator for causal discovery algorithm evaluation. In *33rd Conference on Neural Information Processing Systems (NeurIPS), DEC 08-14, 2019, Vancouver, Canada*, volume 32. Neural Information Processing Systems (NIPS), 2019.

[54] Jill-Jênn Vie and Hisashi Kashima. Knowledge tracing machines: Factorization machines for knowledge tracing. In *Proceedings of the AAAI Conference on Artificial Intelligence*, volume 33, pages 750–757, 2019.

[55] Jussi Viinikka, Antti Hyttinen, Johan Pensar, and Mikko Koivisto. Towards scalable bayesian learning of causal dags. *Advances in Neural Information Processing Systems*, 33:6584–6594, 2020.

[56] Zichao Wang, Sebastian Tschiatschek, Simon Woodhead, José Miguel Hernández-Lobato, Simon Peyton Jones, Richard G Baraniuk, and Cheng Zhang. Educational question mining at scale: Prediction, analysis and personalization. *arXiv preprint arXiv:2003.05980*, 2020.

[57] Zichao Wang, Angus Lamb, Evgeny Saveliev, Pashmina Cameron, Yordan Zaykov, Jose Miguel Hernandez-Lobato, Richard E Turner, Richard G Baraniuk, Craig Barton, Simon Peyton Jones, et al. Results and insights from diagnostic questions: The neurips 2020 education challenge. *arXiv preprint arXiv:2104.04034*, 2021.

[58] Andrew E Waters, David Tinapple, and Richard G Baraniuk. Bayesrank: A bayesian approach to ranked peer grading. In *Proceedings of the Second (2015) ACM Conference on Learning@ Scale*, pages 177–183, 2015.

[59] Ga Wu, Justin Domke, and Scott Sanner. Conditional inference in pre-trained variational autoencoders via cross-coding. *arXiv preprint arXiv:1805.07785*, 2018.

[60] Mike Wu, Milan Mosse, Noah Goodman, and Chris Piech. Zero shot learning for code education: Rubric sampling with deep learning inference. In *Proceedings of the AAAI Conference on Artificial Intelligence*, volume 33, pages 782–790, 2019.

[61] Yue Yu, Jie Chen, Tian Gao, and Mo Yu. Dag-gnn: Dag structure learning with graph neural networks. In *Proceedings of the 36th International Conference on Machine Learning*, 2019.

[62] Bin Zhang, Chris Gaiteri, Liviu-Gabriel Bodea, Zhi Wang, Joshua McElwee, Alexei A Podtelezhnikov, Chunsheng Zhang, Tao Xie, Linh Tran, Radu Dobrin, et al. Integrated systems approach identifies genetic nodes and networks in late-onset alzheimer's disease. *Cell*, 153(3):707–720, 2013.

[63] Xun Zheng, Bryon Aragam, Pradeep Ravikumar, and Eric P. Xing. DAGs with NO TEARS: Continuous Optimization for Structure Learning. In *Advances in Neural Information Processing Systems*, 2018.

[64] Xun Zheng, Chen Dan, Bryon Aragam, Pradeep Ravikumar, and Eric P. Xing. Learning sparse nonparametric DAGs. In *International Conference on Artificial Intelligence and Statistics*, 2020.

## Checklist

1. For all authors...
   (a) Do the main claims made in the abstract and introduction accurately reflect the paper's contributions and scope? [Yes] See last paragraph in Sec. 1
   (b) Did you describe the limitations of your work? [Yes] Include future work at the end of Sec. 5
   (c) Did you discuss any potential negative societal impacts of your work? [N/A]
   (d) Have you read the ethics review guidelines and ensured that your paper conforms to them? [N/A]
2. If you are including theoretical results...
   (a) Did you state the full set of assumptions of all theoretical results? [N/A]
   (b) Did you include complete proofs of all theoretical results? [N/A]
3. If you ran experiments...
   (a) Did you include the code, data, and instructions needed to reproduce the main experimental results (either in the supplemental material or as a URL)? [Yes] We will provide the main model code in the supplemental material. The full running code will be released after acceptance.
   (b) Did you specify all the training details (e.g., data splits, hyperparameters, how they were chosen)? [Yes] See Appx. D
   (c) Did you report error bars (e.g., with respect to the random seed after running experiments multiple times)? [Yes] See Sec. 4
   (d) Did you include the total amount of compute and the type of resources used (e.g., type of GPUs, internal cluster, or cloud provider)? [Yes] See Sec. D.2
4. If you are using existing assets (e.g., code, data, models) or curating/releasing new assets...
   (a) If your work uses existing assets, did you cite the creators? [Yes] The dataset details are in Appx. D, where we cite the creator.
   (b) Did you mention the license of the assets? [N/A]
   (c) Did you include any new assets either in the supplemental material or as a URL? [No]
   (d) Did you discuss whether and how consent was obtained from people whose data you're using/curating? [N/A]
   (e) Did you discuss whether the data you are using/curating contains personally identifiable information or offensive content? [N/A]
5. If you used crowdsourcing or conducted research with human subjects...
   (a) Did you include the full text of instructions given to participants and screenshots, if applicable? [Yes] Only Eedi experiment involves human evaluation and we provide detailed instructions in Sec. 4.3
   (b) Did you describe any potential participant risks, with links to Institutional Review Board (IRB) approvals, if applicable? [N/A]
   (c) Did you include the estimated hourly wage paid to participants and the total amount spent on participant compensation? [N/A]